Polymer 50 (2009) 4626–4634

Contents lists available at ScienceDirect

Polymer

journal homepage: www.elsevier.com/locate/polymer

Fabrication, biomolecular binding, *in vitro* drug release behavior of sugar-installed nanoparticles from star poly(ε-caprolactone)/glycopolymer biohybrid with a dendrimer core

Xiao-Hui Dai [a,b], Hua-Dong Zhang [a], Chang-Ming Dong [a,*]

[a] Department of Polymer Science & Engineering, School of Chemistry and Chemical Engineering, Shanghai Jiao Tong University, Shanghai 200240, PR China
[b] Department of Packaging Engineering, School of Mechanical Engineering, Jiangsu University, Zhenjiang 212013, PR China

ARTICLE INFO

Article history:
Received 16 January 2009
Received in revised form
25 May 2009
Accepted 13 July 2009
Available online 16 July 2009

Keywords:
Star copolymers with a dendrimer core
Glycopolymers
Self-assembly

ABSTRACT

Star poly(amido amine)-b-poly(ε-caprolactone)-b-poly(D-gluconamidoethyl methacrylate) (PAMAM–PCL–PGAMA) block copolymers with a dendrimer core were synthesized from the ring-opening polymerization of ε-caprolactone using a hydroxyl-terminated dendrimer poly(amido amine) initiator followed by the direct atom transfer radical polymerization of unprotected glycomonomer. The self-assembly and the biomolecular binding of PAMAM–PCL–PGAMA with Concanavalin A (Con A) were investigated by NMR, UV–vis, dynamic light scattering, and transmission electron microscopy, respectively. Multivalent sugar-installed vesicles and large compound aggregates were self-assembled from these dendritic copolymers in aqueous solution, demonstrating thermodynamically more stable than those self-assembled from linear counterpart. Moreover, these copolymers presented specific biomolecular binding with Con A lectin compared with bovine serum albumin, while both the lower mobility and the higher spatial hindrance within dendritic copolymers, to some extent, limited the clustering between sugar and Con A. Furthermore, these star copolymer nanoparticles showed a higher drug-loading efficiency and less burst release compared with linear counterpart. This work provides a method not only for the synthesis of star PCL/glycopolymer biohybrid with a dendrimer core but also for the fabrication of sugar-installed nanoparticles with tunable clustering ability, good drug-loading efficiency, and controlled drug-release profile useful for targeted drug delivery system.

1. Introduction

In contrast to small molecular surfactant micelles and liposomes, polymeric nanoparticles with tunably physicochemical and biological surfaces (e.g., micelles and vesicles) have been widely investigated for drug/gene delivery systems because they cannot only improve the solubility of hydrophobic drugs, but also protect protein drugs/genes from digestion, demonstrating a long blood circulation time and an accumulation in diseased tissues/organs via enhanced permeability and retention effect [1–5]. However, the passive accumulation effect at tumor sites may be compromised by the slightly higher hydrostatic pressure in tumor extracellular space than normal tissues [6]. Even more, owing to their limited permeability or mobility and non-specific interactions with extracellular matrix, most nanoparticles often block the leaky sites of tumor blood vessels, hindering the subsequent intracellular translocation. Indeed, combining both passive and active targeting approaches with polymeric nanoparticles attracted much attention in current tumor therapy [7]. For instance, utilization of the biomolecular antibody–antigen recognition has been intensively investigated for the fabrication of targeted drug delivery system [8,9]. However, this approach has some shortcomings such as the immunogenicity and the high cost of antibody in production, which limited its clinical applications. Thus, developing novel tumor targeting methods is still important for cancer therapy and nanomedicine.

Recently, multivalent sugar–protein binding (i.e., biomolecular binding) in cells/viruses/toxins has been intensively investigated for the fabrication of sugar-related biosensors, arrays or chips, and sugar-surfaced nanoparticles [10,11]. As the biomimetics of natural polysaccharides, well-defined glycopolymers (side-chain sugar-containing polymers) provide a versatile strategy for the fabrication of sugar-installed nanoparticles useful for targeted drug/gene delivery. For example, sugar-installed polymeric micelles (i.e., micelles having sugar residues on the surface) and vesicles were conveniently generated by the self-assembly of amphiphilic

* Corresponding author. Tel.: +86 21 54748916; fax: +86 21 54741297.
E-mail address: cmdong@sjtu.edu.cn (C.-M. Dong).

0032-3861/$ – see front matter © 2009 Elsevier Ltd. All rights reserved.
doi:10.1016/j.polymer.2009.07.017

glycopolymers with different macromolecular architectures [12–21]. On the other hand, biodegradable biomaterial such as poly(ε-caprolactone) (PCL) has been widely used in pharmacological and biomedical fields [21–23]. Therefore, combining hydrophobic PCL and water-soluble glycopolymer with dendritic architecture will provide a facile strategy for the preparation of amphiphilic dendritic PCL/glycopolymer biohybrids, importantly, new physicochemical properties can be endowed with these biohybrids by tuning both the compositions and the macromolecular architecture.

Herein, star block copolymers composed of biodegradable PCL and glycopolymer were synthesized from the ring-opening polymerization (ROP) of ε-caprolactone using a hydroxyl-terminated dendrimer poly(amido amine) initiator followed by the direct atom transfer radical polymerization (ATRP) of unprotected glycomonomer, as shown in Scheme 1. The molecular structures, self-assembly, biomolecular recognition, and drug release behavior of these copolymers were thoroughly investigated by means of FT-IR, NMR, gel permeation chromatography, differential scanning calorimetry, wide angle X-ray diffraction, dynamic light scattering, and transmission electron microscopy. The star biohybrid with a dendrimer core self-assembled into thermodynamically more stable nanoparticles than those of both linear and star-shaped counterparts in aqueous solution, suggesting a longer blood circulation time for drug delivery [2,21,24]. To evaluate their feasibility as nanocarrier for drugs, nimodipine (Scheme 2), a second-generation dihydropyridine calcium antagonist with apparent selectivity for cerebral blood vessels [25], was selected as a model hydrophobic drug to incorporate into the sugar-installed nanoparticles. Significantly, this provides a method not only for the synthesis of star PCL/glycopolymer biohybrid with a dendrimer core but also for the fabrication of sugar-installed nanoparticles with tunable clustering ability, good drug-loading efficiency, and controlled drug-release profile useful for targeted drug delivery system.

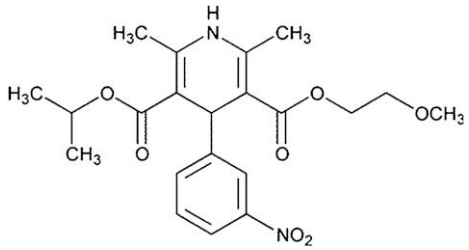

Scheme 2. The chemical structure of nimodipine.

2. Experimental section

2.1. Materials

2-Aminoethyl methacrylate hydrochloride, bipyridine, 2-bromo-2-methylpropionyl bromide, copper (I) bromide, 1,6-diphenyl-1,3,5-hexatriene (DPH), D-gluconolactone, and stannous octoate ($SnOct_2$) were purchased from Aldrich or Acros and used as-received. ε-Caprolactone (CL, Aldrich) and toluene were distilled from CaH_2, respectively. Concanavalin A (Con A) lectin and bovine serum albumin (BSA) were purchased from Sigma. D-Gluconamidoethyl methacrylate glycomonomer (GAMA) was synthesized from D-gluconolactone and 2-aminoethyl methacrylate hydrochloride according to our previous publication [21]. Hydroxyl-terminated

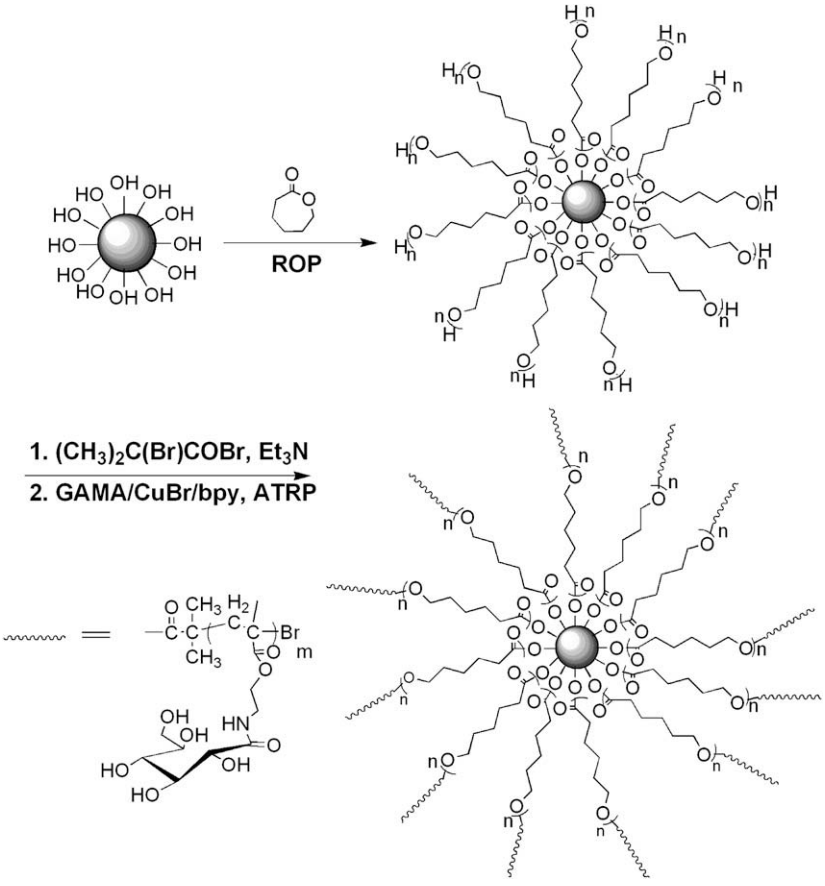

Scheme 1. Synthesis of dendritic PAMAM–PCL–PGAMA block copolymers.

poly(amido amine) (PAMAM–OH) with twelve hydroxyl terminal groups was synthesized according to the literature procedure [26]. ^{1}H NMR ($CDCl_3$) of PAMAM–OH: 7.56 (NH, bt, 4H), 3.57 ($CONHCH_2$, s, 24H), 2.63 (NCH_2CH_2CO, t, 8H), 2.46 (NCH_2CH_2N, bt, 4H), 2.30 (NCH_2CH_2CO, t, 8H).

2.2. Methods

Fourier transform infrared (FT-IR) spectra were recorded on a Perkin Elmer Paragon 1000 spectrometer at frequencies ranging from 400 to 4000 cm^{-1}. Samples were thoroughly mixed with KBr and pressed into pellet form. Molecular weight and molecular weight distribution (M_w/M_n) of polymer were determined on a gel permeation chromatograph (GPC, Perkin–Elmer Series 200) and a refractive index detector at 30 °C. The elution phase was DMF (0.01 mol/L LiBr) (elution rate: 1.0 mL/min), and polystyrene was used as the calibration standard. ^{1}H NMR spectra (400 MHz) were recorded at room temperature on a Varian Mercury-400 spectrometer. The differential scanning calorimetry (DSC) analysis was carried out using a Perkin–Elmer Pyris 1 instrument under nitrogen flow (10 mL/min). All samples were heated from 25 °C to 160 °C at 10 °C/min. UV–vis spectra were recorded at room temperature using a Spectrumlab54 UV–visible spectrophotometer. The mean size of aggregates was determined by dynamic light scattering (DLS) using a Malvern Nano_S instrument (Malvern, UK). The solution of aggregates (0.5 mg/mL) was performed at a scattering angle of 90 °C and at 25 °C. The particle size distributions were computed using cumulants analysis by Dispersion Technology Software 4.00 (Malvern). All the measurements were repeated three times, and the average values reported were the mean diameter ± standard deviation. Transmission electron microscopy (TEM) was performed using a JEM-2010/INCA OXFORD TEM (JEOL/OXFORD) at a 200 kV accelerating voltage. One drop of aggregates solution was deposited onto the surface of 300 mesh Formvar-carbon film-coated copper grids. Excess solution was quickly wicked away with a filter paper. The image contrast was enhanced by negative staining with phosphotungstic acid (0.5 wt.%).

2.3. Preparation of 2-bromo-2-methylpropionyl-terminated star poly(amido amine)-b-poly(ε-caprolactone) (PAMAM–PCL–Br) for ATRP

Star poly(amido amine)-b-poly(ε-caprolactone) with twelve hydroxyl end groups (PAMAM–PCL) was synthesized by the controlled ring-opening polymerization of ε-caprolactone using PAMAM–OH as an initiator and stannous octoate as a catalyst at 120 °C. A typical procedure follows: 2.2 mg (5.4 μmol) of the $SnOct_2$ catalyst was added to the melt mixture of the PAMAM–OH initiator (5.7 mg, 0.017 mmol) and CL monomer (0.3 mL, 2.7 mmol). The polymerization was carried out in bulk at 120 °C for 24 h. Then, the resulting product was dissolved in 5 mL of CH_2Cl_2 and poured dropwise into 50 mL of cold methanol under vigorous stirring at room temperature. The precipitate was filtered and dried in vacuo at 40 °C to give 276.2 mg of the PAMAM–PCL_{28} sample (91% yield). ^{1}H NMR ($CDCl_3$) of PAMAM–PCL_{28} sample: δ (ppm) = 1.35–1.43 (m, 672H, $COCH_2CH_2CH_2CH_2CH_2O$), 1.53–1.72 (m, 1344H, $COCH_2CH_2CH_2CH_2CH_2O$), 2.25–2.41 (m, 672H, $COCH_2CH_2CH_2CH_2CH_2O$), 3.65 (t, 24H, CH_2OH), 4.03–4.15 (m, 672H, $COCH_2CH_2CH_2CH_2CH_2O$). Then, the PAMAM–PCL_{28} precursor was converted into ATRP macroinitiator via esterification with 2-bromo-2-methylpropionyl bromide. A typical example is given below. PAMAM–PCL_{28} precursor (566.1 mg, 0.015 mmol) was dissolved in dry CH_2Cl_2 (15 mL). To this solution was added triethylamine (0.8 mmol, 112 μL) under N_2, and the reaction mixture was stirred for 30 min and then cooled to 0 °C. 2-Bromo-2-methylpropionyl bromide (0.72 mmol, 91 μL) in CH_2Cl_2 (10 mL) was added dropwise to PAMAM–PCL_{28} solution via a syringe under N_2 and kept 1 h at 0 °C. The reaction was stirred vigorously for 36 h at room temperature, and then the mixture was washed sequentially with saturated $NaHCO_3$ solution and distilled water. The organic layer was dried over anhydrous Na_2SO_4, and most of the solvent was removed using a rotary evaporator. The residue was precipitated dropwise into cold methanol, and then dried in vacuo at 50 °C for 24 h (83% yield). ^{1}H NMR ($CDCl_3$) of PAMAM–PCL_{28}–Br sample: δ (ppm) = 1.32–1.49 (m, 672H, $COCH_2CH_2CH_2CH_2CH_2O$), 1.54–1.77 (m, 1344H, $COCH_2CH_2CH_2CH_2CH_2O$), 1.93 (s, 72H, $C(CH_3)_2Br$), 2.25–2.41 (m, 672H, $COCH_2CH_2CH_2CH_2CH_2O$), 4.02–4.16 (m, 672H, $COCH_2CH_2CH_2CH_2CH_2CH_2O$).

2.4. Synthesis of star PAMAM–PCL–PGAMA block copolymers

Star poly(amido amine)-b-poly(ε-caprolactone)-b-poly(D-gluconamidoethyl methacrylate) (PAMAM–PCL–PGAMA) was synthesized by the direct ATRP of unprotected GAMA glycomonomer using PAMAM–PCL_{28}–Br macroinitiator in NMP at room temperature. A typical procedure is as follows: both PAMAM–PCL_{28}–Br macroinitiator (0.5 μmol, 19.8 mg) and GAMA glycomonomer (0.36 mmol, 110.7 mg) were dissolved in NMP (0.6 mL) at room temperature, and the mixture solution was degassed via nitrogen purge for 30 min. Copper (I) bromide (6 μmol, 0.9 mg) and bipyridine (12 μmol, 1.9 mg) were added in turn, and the resulting solution was degassed again for 10 min. and then stirred vigorously under nitrogen at room temperature for 24 h. The mixture was precipitated into isopropanol (20 mL), and then purified sequentially by THF (4 mL) and heated methanol (5 mL) to remove the possible unreacted macroinitiator and GAMA glycomonomer. The resulting block copolymer was then dried in vacuo overnight at 40 °C (49% yield).

2.5. Measurement of copolymer critical aggregation concentration

The critical aggregation concentration (cac) of amphiphilic PAMAM–PCL–PGAMA copolymers was determined employing the hydrophobic dye solubilization method using DPH as a probe molecule according to the literature [27]. UV–vis spectra of samples were recorded in the range of 200–500 nm at room temperature.

2.6. Preparation of nimodipine-loaded nanoparticles in water

Both star PAMAM–PCL–PGAMA copolymer (8.9 mg) and nimodipine (2.4 mg) were dissolved in 6 mL of DMF and stirred vigorously for 24 h at room temperature. The resulting solution was loaded into a dialysis bag with a molecular weight cut-off (MWCO) of 7000 Da, and then dialyzed against distilled water for 3 days to form drug-loaded nanoparticles solution. The nimodipine loading content was analyzed by UV–vis at 372 nm. The nimodipine drug-loading efficiency of nanoparticles is calculated as the ratio of actual and added drug content. Similarly, the blank nanoparticles were also fabricated in aqueous solution. Both the mean size and morphology of nanoparticles were determined by DLS and TEM, respectively.

2.7. Qualitative lectin recognition assay

The qualitative lectin recognition activity of the copolymer solution was analyzed by changes in the turbidity of solution with time at 360 nm and room temperature following the addition of various concentrations of aggregate solution into Con A solution, in which its concentration was equal to 0.5 mg/mL. Similarly, BSA was used for the control experiments.

2.8. Quantitative lectin recognition assay

According to the literature [28,29], the nanoparticles stock solution was diluted into a series of solution ($C = 10^{-3}$–0.08 mg/mL) for quantitative lectin recognition assays. The assay was performed at 22 °C in 0.1 M Tris/HCl buffer, pH 7.2, containing 0.15 M NaCl, 1 mM $CaCl_2$ and 1 mM $MnCl_2$. Con A (500 μL, 0.5 mg/mL) was added to 500 μL of the nanoparticles solution. The mixtures were allowed to sit for 24 h. The solutions were centrifuged for 5 min (5000 rpm) to pellet the precipitate. The concentration of unbound Con A in each solution was determined by UV–vis at 280 nm. The values given are the average of three independent measurements.

2.9. In vitro drug release from nimodipine-loaded nanoparticles

The drug-loaded nanoparticles solution in a dialysis bag with MWCO of 7000 Da were directly immersed into 400 mL of distilled water at 37 °C. The drug-released solution (5 mL) was changed periodically, and the amount of nimodipine released from nanoparticles was measured by UV–vis at 372 nm at room temperature. All release experiments were carried out in duplicate, and all data were averages of three determinations used for drawing figures.

3. Results and discussion

3.1. Synthesis of star PAMAM–PCL–PGAMA block copolymers

From a synthetic viewpoint, linear poly(ε-caprolactone)/glycopolymer block copolymers can be synthesized via the controlled ring-opening polymerization (ROP) of ε-caprolactone (CL), the "living" terminal group transformation, the atom transfer radical polymerization (ATRP) of a protected glycomonomer, followed by the deprotection of glycopolymer segment [30–38]. In this work, star poly(amido amine)-b-poly(ε-caprolactone)-b-poly(D-gluconamidoethyl methacrylate) (PAMAM–PCL–PGAMA) block copolymers with a dendrimer core were rationally synthesized from the ROP of CL using a dendritic hydroxyl-terminated poly(amido amine) (PAMAM–OH) initiator, the "living" terminal group transformation, followed by the direct atom transfer radical polymerization (ATRP) of unprotected glycomonomer, as shown in Scheme 1. This methodology precludes the possible degradation of biodegradable PCL segment without vigorous deprotection step. Firstly, star PAMAM–PCL with twelve hydroxyl end groups (PAMAM–PCL) was synthesized by the controlled ROP of CL monomer using a dendritic PAMAM–OH initiator and $SnOct_2$ catalyst at 120 °C. Comparing the ^{1}H NMR spectrum of PAMAM–PCL with that of PAMAM–OH initiator (Supporting information, Fig. S1), the proton signals assignable to PAMAM initiator appeared within PAMAM–PCL, and the single proton signal assignable to CH_2-OH sites of PAMAM–OH completely disappeared. This suggests that all the OH groups of dendrimer PAMAM–OH initiated the ROP of CL. The actual polymer molecular weight of PAMAM–PCL ($M_{n,NMR}$) could be easily determined by means of ^{1}H NMR spectroscopy, which was in good agreement with the theoretically calculated molecular weight (i.e., $M_{n,th}$, $M_{n,th} = M_{initiator} + [M]/[I] \times M_{CL} \times$ yield, Table 1). The GPC curves of PAMAM–PCL polymers gave symmetrical and unimodal peaks, shifting up to higher molecular weight regions with the increasing PCL block length (Fig. 1). Then PAMAM–PCL was further reacted with 2-bromo-2-methylpropionyl bromide to introduce active initiating species for ATRP. As a representative example, the ^{1}H NMR of the resulting PAMAM–PCL_{28}–Br macroinitiator gave a new proton signal at 1.94 ppm, corresponding to methyl of 2-bromo-2-methylpropionate, while the proton signal at 3.65 ppm assignable to the primary hydroxy methylene end group ($HOCH_2$) of PAMAM–PCL wholly disappeared (Supporting information, Fig. S2).

Table 1
Synthesis of linear PCL (LPCL) and dendritic PAMAM–PCL using $SnOct_2$ as catalyst in bulk at 120 °C.

Entry[a]	$[M]/[I]$[b]	$M_{n,th}$[c]	$M_{n,NMR}$[d]	$M_{n,GPC}$[e]	M_w/M_n[e]	Yield (%)
$LPCL_{28}$[f]	58:1	6300	6510	10 290	1.21	95.2
PAMAM–PCL_{17}	240:1	23 550	24 040	15 850	1.69	83.2
PAMAM–PCL_{28}	360:1	36 020	37 740	20 330	1.46	85.8

[a] The subscript number represents the degree of polymerization (DP) of PCL block, in which $DP = S_d/S_e$, and S denotes integral of proton signal, as shown in Fig. S1.
[b] M = CL, I = initiator.
[c] $M_{n,th} = M_{initiator} + [M]/[I] \times M_{CL} \times$ Yield, $M_{n,th}$ denotes the theoretical number-average molecular weight of PCL polymer.
[d] $M_{n,NMR}$ was determined from the integral ratio of the signal on the main chain of polymer (CH_2, $\delta = 2.10$–2.40 ppm) and the signal on the primary hydroxy methylene end group ($HOCH_2$, $\delta = 3.65$ ppm).
[e] Weight-average molecular weight (M_w) and number-average molecular weight (M_n) are determined by GPC.
[f] LPCL denotes the linear PCL synthesized using1,6-hexanediol as an initiator [21].

Moreover, the integral ratio of the proton signal on 2-bromo-2-methylpropionate terminal group to the repeating methylene unit (CH_2) of PAMAM–PCL_{28}–Br was in good agreement with the theoretical value ($H^a/H^f = 56/6$). These results demonstrate that the hydroxyl terminal groups of PAMAM–PCL precursor were quantitatively converted into ATRP initiating species within PAMAM–PCL–Br.

Using PAMAM–PCL–Br as the macroinitiator, the direct ATRP of unprotected GAMA glycomonomer was performed in NMP solution at room temperature. The detailed results are summarized in Table 2. Compared with that of the PAMAM–PCL precursor, the typical GPC curves of PAMAM–PCL–PGAMA copolymers revealed symmetrical elution peaks at different elution times, denoting a progression of polymer molecular weight and narrow polydispersity (Fig. 1). This result convincingly confirmed the successful synthesis of purified star PAMAM–PCL–PGAMA block copolymers. Note that these star copolymers gave much underestimated molecular weights ($M_{n,GPC}$s) than their actual molecular weights ($M_{n,NMR}$s), which could be attributed to their smaller hydrodynamic volume and strong molecular interactions within copolymers [39–41]. As a representative example, the ^{1}H NMR (DMSO-d_6) of PAMAM–PCL–PGAMA clearly shows that besides the typical proton signals of PCL backbone, new proton signals appeared at 3.3–4.6 ppm for glucose residues, and at both 1.86 ppm and 0.6–1.0 ppm for the backbone of PGAMA glycopolymer (Fig. 2a). The actual molecular weight of

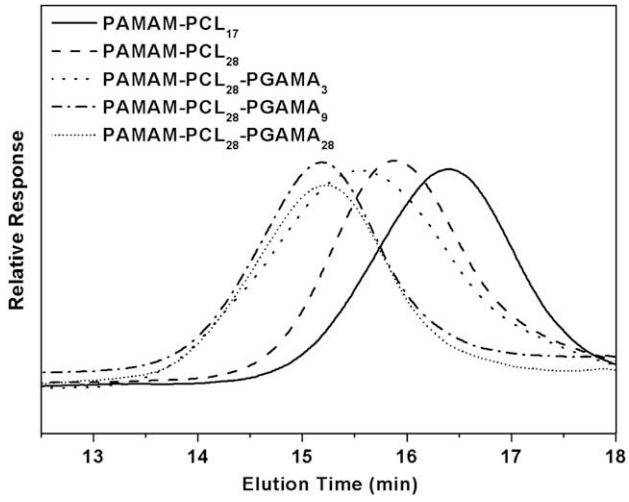

Fig. 1. GPC traces of PAMAM–PCL and PAMAM–PCL–PGAMA block copolymers in DMF solution.

Table 2
Synthesis of linear LPCL–PGAMA and dendritic PAMAM–PCL–PGAMA block copolymers via the direct ATRP of GAMA monomer in NMP solution at room temperature.

Entry[a]	[GAMA]/[I]	$M_{n,GPC}$	M_w/M_n	$M_{n,NMR}$[b]	f_{PCL}/f_{PGAMA}[c] %/%)
$LPCL_{28}$–$PGAMA_3$	10	14 920	1.25	8350	78/22
$LPCL_{28}$–$PGAMA_{28}$	100	23 610	1.17	23 740	27/73
PAMAM–PCL_{28}–$PGAMA_3$	60	24 750	1.37	45 470	79/21
PAMAM–PCL_{28}–$PGAMA_9$	360	26 530	1.29	68 250	53/47
PAMAM–PCL_{28}–$PGAMA_{28}$	900	25 900	1.31	139 330	26/74

[a] The subscript numbers represent the degree of polymerization of PCL and PGAMA blocks.
[b] $M_{n,NMR}$ was determined from the integral ratio of the signal on the main chain of PCL (–CH_2–, 2.20–2.29 ppm) and the signal on the main chain of PGAMA (–CH_2–, 1.86 ppm) (e.g., the ^{1}H NMR of Fig. 2A).
[c] f denotes the weight fractions of PCL and/or PGAMA within block copolymers, which was determined by ^{1}H NMR.

these block copolymers ($M_{n,NMR}$) could be determined by ^{1}H NMR, and the PGAMA block length can be controlled by the molar ratio of GAMA glycomonomer to PAMAM–PCL–Br macroinitiator. Moreover, compared with that of PAMAM–PCL precursor, FT-IR spectra of PAMAM–PCL–PGAMA copolymers present the characteristic amide I band at 1643 cm^{-1} (overlapped with PAMAM) and amide II band at 1542 cm^{-1} for the linker groups within PGAMA block (Fig. 3). Meanwhile, the relative intensities of carbonyl band at 1731 cm^{-1} within PCL block to the amide I band within both PAMAM and PGAMA blocks decreased gradually with the increasing block length of PGAMA. Furthermore, the DSC analysis of these star copolymers demonstrated that the outer PGAMA block

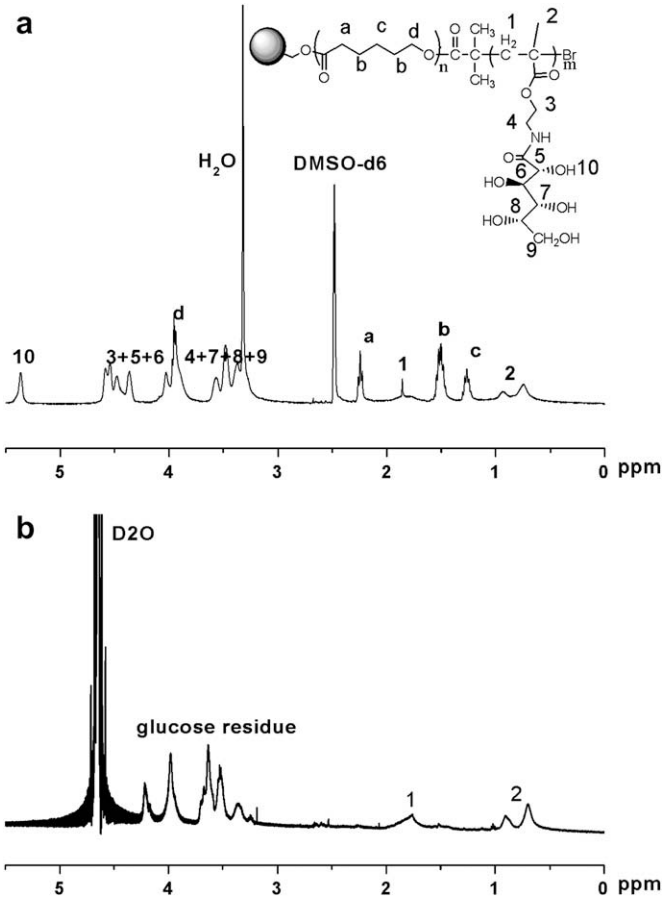

Fig. 2. ^{1}H NMR spectra of PAMAM–PCL_{28}–$PGAMA_{28}$ sample in d_6-DMSO (a) and D_2O (b).

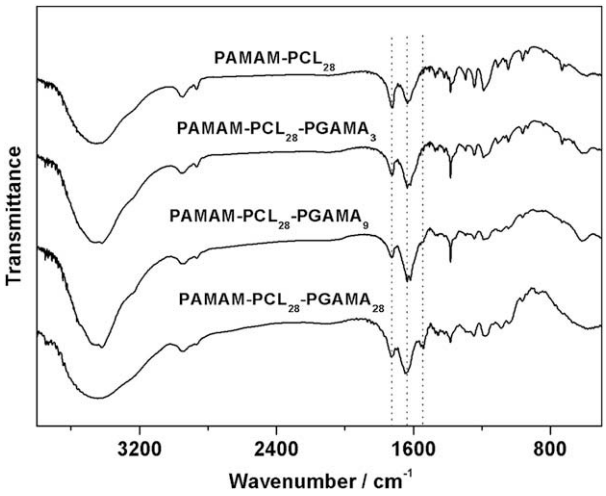

Fig. 3. FT-IR spectra of PAMAM–PCL and PAMAM–PCL–PGAMA copolymers.

progressively hampered the crystallization of the inner PCL block, and the degree of crystallinity (X_c) of the PCL block decreased dramatically from 61.3% to 30.2% with the increasing block length of PGAMA, as shown in Table 3 and Supporting information, Fig. S3. In all, the above results demonstrate that star PAMAM–PCL–PGAMA block copolymers with a dendrimer core were successfully synthesized via combining ROP of CL monomer and direct ATRP of unprotected GAMA glycomonomer (Scheme 1).

3.2. Fabrication of sugar-installed nanoparticles via self-assembly

Using a well-known dialysis method [21,42], the sugar-installed and PCL-cored nanoparticles were fabricated via the self-assembly of these star copolymers in aqueous solution. Firstly, the self-assembly behavior of star PAMAM–PCL–PGAMA block copolymers was characterized by ^{1}H NMR (Fig. 2b). Compared with that in d_6-DMSO solution (Fig. 2a), the ^{1}H NMR of PAMAM–PCL_{28}–$PGAMA_{28}$ in D_2O solution gave the nearly negligible proton signals of hydrophobic PCL segments. This phenomenon could be attributed to both the decreased mobility of aggregated PCL blocks and the shielding effect of hydrophilic PGAMA shell to the hydrophobic PCL core [18,19]. This result also implies the spontaneous self-assembly of star PAMAM–PCL–PGAMA copolymers in aqueous solution. Then, their critical aggregation concentration (cac) was determined by using the dye solubilization method [27], as shown in Fig. 4. The absorbance intensity of DPH dye remained nearly constant below a certain concentration, and then increased substantially, reflecting the incorporation of DPH in the hydrophobic core of nanoparticles. The cac value of PAMAM–PCL–PGAMA copolymers (about 0.006 mg/mL) was order of magnitude lower than that of linear

Table 3
Thermal properties of dendritic PAMAM–PCL–PGAMA block copolymers.

Sample	T_m[a] (°C)	ΔH_m[b] (J/g)	X_c (%)[c]
PAMAM–PCL_{28}	56.0	85.6	61.3
PAMAM–PCL_{28}–$PGAMA_3$	55.6	49.2	44.6
PAMAM–PCL_{28}–$PGAMA_9$	55.0	28.1	38.2
PAMAM–PCL_{28}–$PGAMA_{28}$	52.5, 58.2	10.9	30.2

[a] T_m denotes the maximal melting temperature of PCL block within copolymer in the heating run.
[b] ΔH_m denotes the fusion enthalpy of PCL block within copolymer in the heating run.
[c] X_c denotes the degree of crystallization of PCL block within copolymer, and $X_c = \Delta H_m/(f_{PCL} \times \Delta H^0_{m,PCL})$, $\Delta H^0_{m,PCL} = 139.6$ J/g.

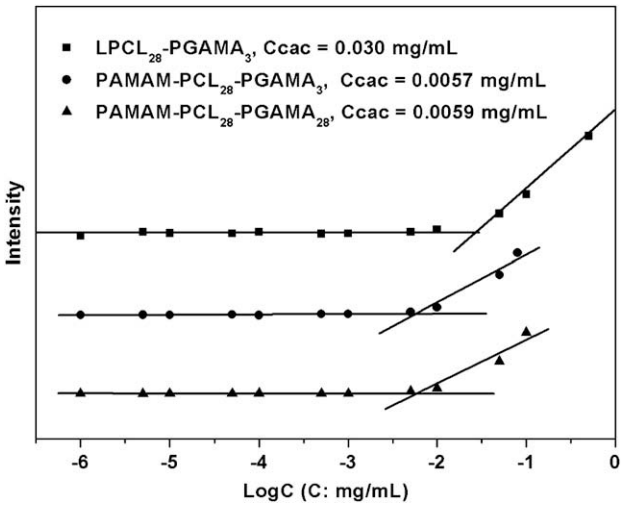

Fig. 4. The relationship of the absorbance intensity of DPH as a function of copolymer concentration at room temperature.

counterpart (0.03 mg/mL). This suggests that the star copolymers with a dendrimer core self-assembled into thermodynamically more stable nanoparticles than the linear counterpart in aqueous solution, providing potentially a longer blood circulation time for drug delivery [2,21,24]. Note that the cac value of PAMAM–PCL_{28}–$PGAMA_3$ is very close to that of PAMAM–PCL_{28}–$PGAMA_{28}$. This is attributable to the fact that the star copolymers with a dendrimer core have a tendency to form unimolecular micelles, and the hydrophilic composition of copolymer usually has slight effect on it [2,24].

Both the morphology and the average size of the self-assembled aggregates from these star copolymers were investigated by the techniques of TEM and DLS, as shown in Fig. 5 and Fig. 6. To investigate the effect of hydrophilic PGAMA block length and/or the weight fraction (f_{PGAMA}) on the nanoparticles' morphology, the hydrophobic PCL block was kept equal to 28 repeating units. When the PGAMA block was short (e.g., PAMAM–PCL_{28}–$PGAMA_3$, $f_{PGAMA} = 21\%$), the bilayered vesicles or polymersomes (about 102.2 ± 1.8 nm) were obtained in Figs. 5A and 6A. As the PGAMA block length increased up to 9 ($f_{PGAMA} = 47\%$), the normally spherical micelles with a diameter of about 146.3 ± 2.3 nm were presented for PAMAM–PCL_{28}–$PGAMA_9$ sample (Figs. 5B and 6B). With the continuous increasing PGAMA length, the large compound

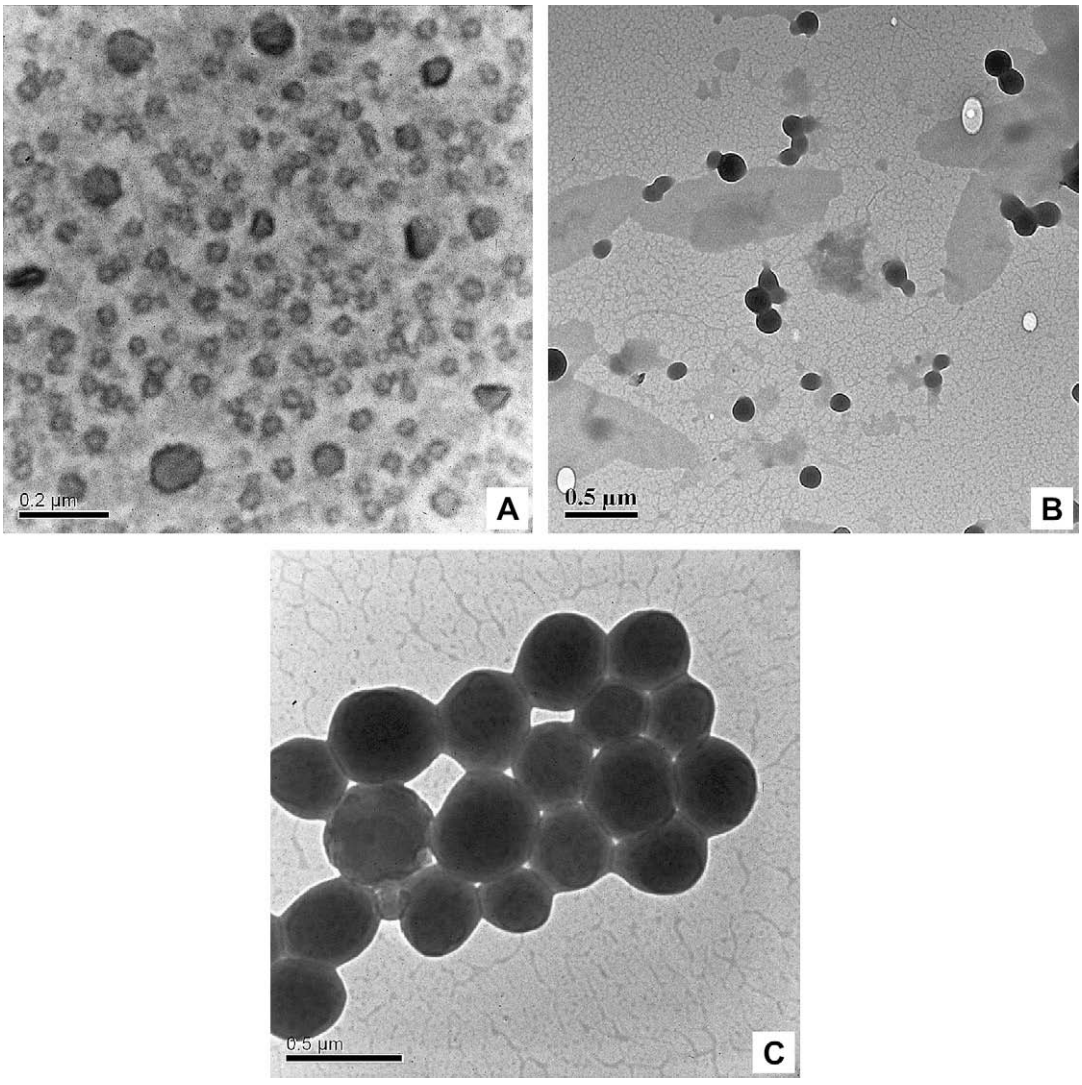

Fig. 5. TEM photographs of copolymers nanoparticles: PAMAM–PCL_{28}–$PGAMA_3$ (A), PAMAM–PCL_{28}–$PGAMA_9$ (B), and PAMAM–PCL_{28}–$PGAMA_{28}$ (C).

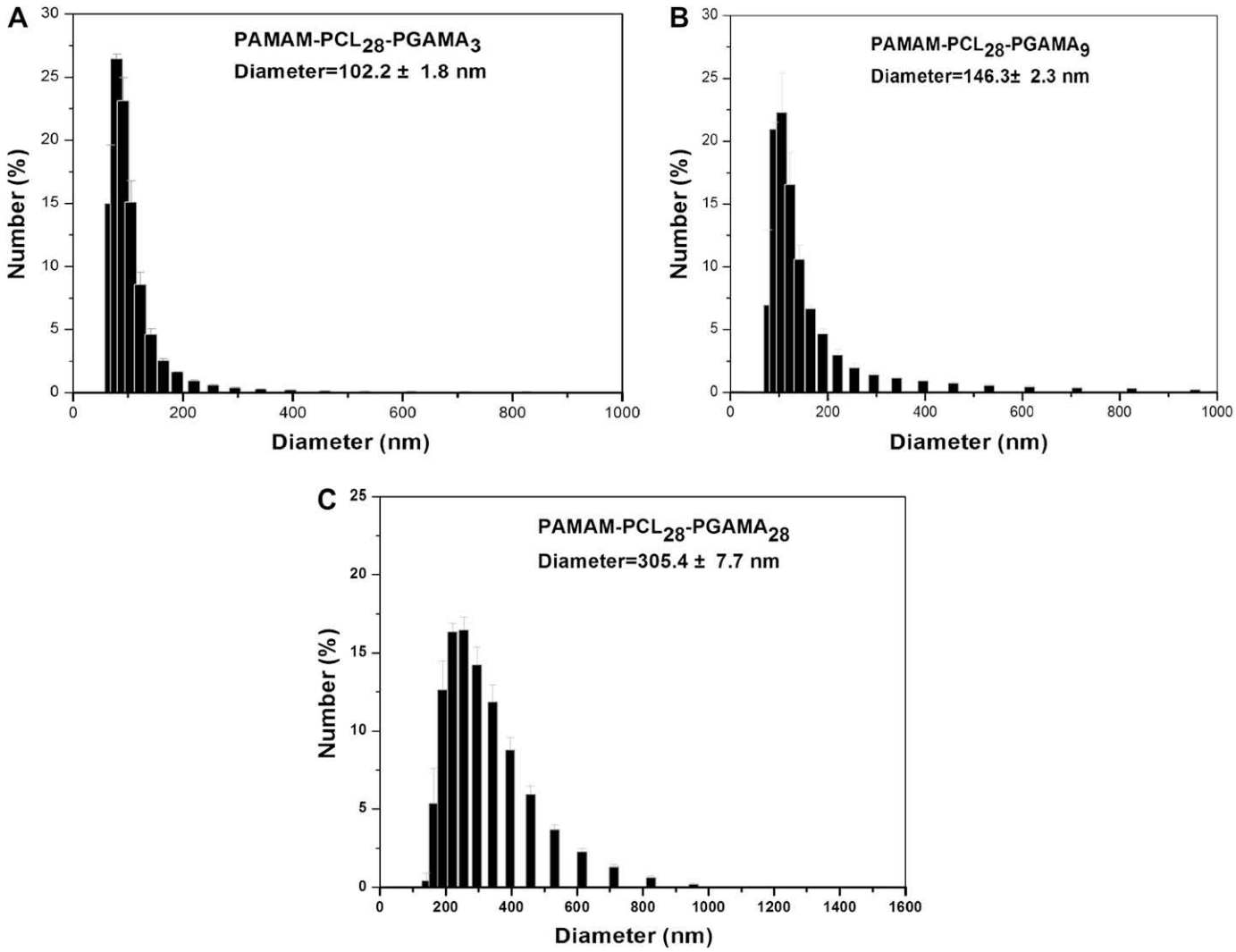

Fig. 6. Nanoparticles size distribution of copolymers in aqueous solution: PAMAM–PCL_{28}–$PGAMA_3$ (A), PAMAM–PCL_{28}–$PGAMA_9$ (B), and PAMAM–PCL_{28}–$PGAMA_{28}$ (C).

aggregates (about 305.4 ± 7.7 nm) were fabricated for PAMAM–PCL_{28}–$PGAMA_{28}$ sample ($f_{PGAMA} = 74\%$, Figs. 5C and 6C). These larger sugar-installed aggregates are possibly formed by the inter-micellar aggregation of the normal micelles (10–50 nm) [21,24], being induced by the strong hydrogen-bond interactions among the glycopolymer shell, which needs further investigation. Similar large compound aggregates have been observed by TEM for both amphiphilic block copolymers such as polystyrene-b-poly[2-(β-D-glucopyranosyloxy)ethyl acrylate] and polystyrene-b-poly(acrylic acid) in literature [13,43]. These results indicate that the sugar-installed nanoparticles with micellar and vesicular morphologies could be fabricated by adjusting the weight fraction of PGAMA block within these star copolymers.

3.3. Recognition properties of star PAMAM–PCL–PGAMA block copolymers

Multivalent sugar-containing ligands (e.g., glycopolymer and glycodendrimer) can cluster receptors on cell-surface, viruses, toxins, and lectins, exhibiting a specific multivalent interaction for the fabrication of targeted drug delivery systems [10,11,28,29]. Concanavalin A (Con A) lectin specifically recognizes D-glucopyranoside and D-mannopyranoside residues with free 3-, 4-, and 6-

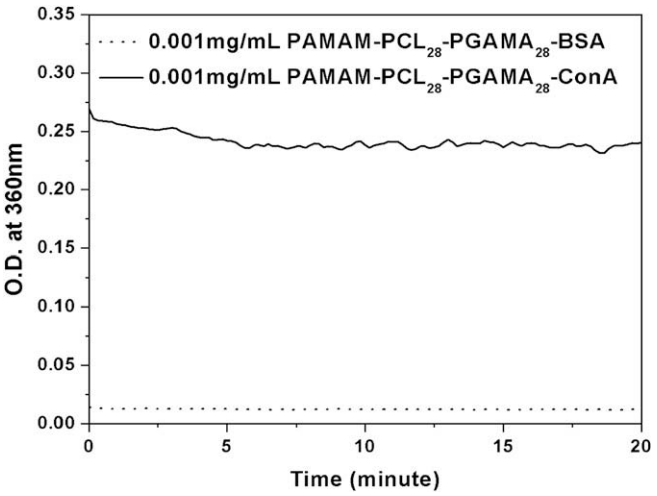

Fig. 7. The qualitative binding assay of Con A ($C = 0.5$ mg/mL) or BSA ($C = 0.5$ mg/mL) with PAMAM–PCL_{28}–$PGAMA_{28}$ ($C = 0.001$ mg/mL).

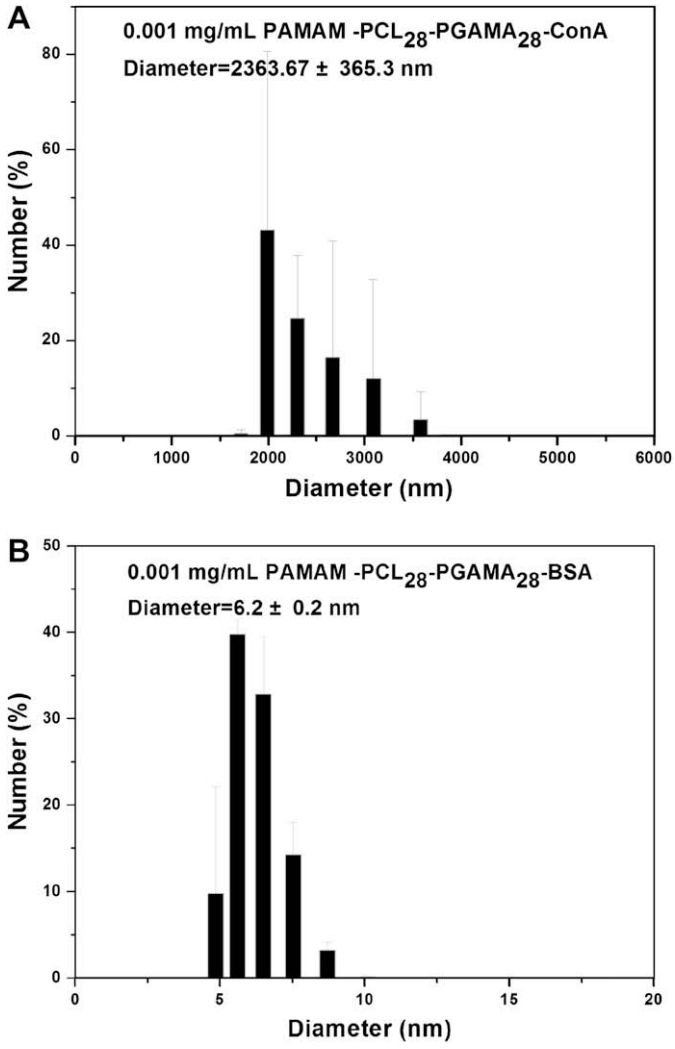

Fig. 8. Nanoparticle size distribution of PAMAM–PCL_{28}–$PGAMA_{28}$–Con A mixed solution (A) and PAMAM–PCL_{28}–$PGAMA_{28}$–BSA mixed solution (B).

hydroxyl groups, and the binding of Con A with glycopolymer usually results in the Con A/glycopolymer cross-linked aggregates [13,21]. The qualitative binding assay of Con A with star PAMAM-PCL–PGAMA copolymer was investigated by UV–vis, as shown in Fig. 7. The turbidity of the copolymer solution increased after Con A was added, while nearly no change was observed after BSA was added. This result suggests that the specific binding between star copolymer and Con A occurred and probably resulted in the Con A/copolymer cross-linked aggregates, which was supported by the following DLS analysis. The average size of the Con A/copolymer cross-linked aggregates was about 2633.7 ± 365.3 nm, which was much bigger than the original copolymer aggregates (about 305.4 ± 7.7 nm), as shown in Fig. 8A. However, the BSA/copolymer mixed solution showed the nanoparticles with a diameter of about 6.2 ± 0.2 nm (Fig. 8B), which is consistent with the size of BSA molecules in solution ($C_{BSA} = 0.5$ mg/mL ≫ Ccopolymer = 0.001 mg/mL). This result indicates that no binding between the star copolymer and BSA occurred in aqueous solution at room temperature.

Whether does star architecture of copolymer have effect on the binding with Con A? The quantitative binding assay was further determined by UV–vis, as shown in Fig. 9. The amount of Con A clustering increased over that of linear copolymer, and then kept

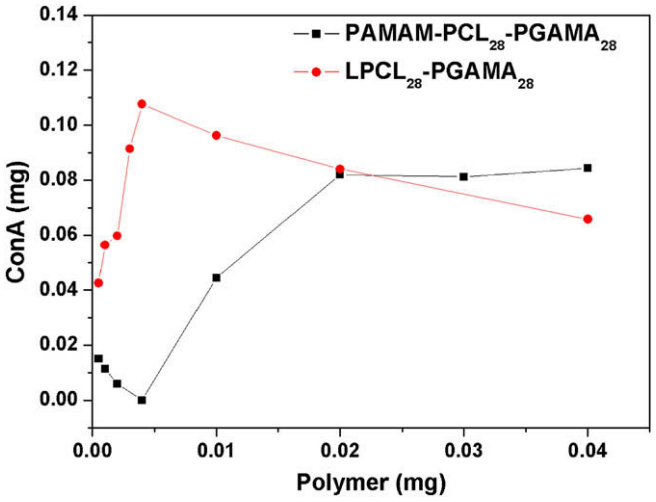

Fig. 9. The quantitative binding assay of Con A ($C = 0.5$ mg/mL) with PAMAM–PCL_{28}–$PGAMA_{28}$ ($C = 0.001$–0.08 mg/mL).

nearly unchanged. Note that the amount of Con A clustering with star copolymer attained a maximum, and then decreased a little over that of copolymer (Ccopolymer = 0.001–0.08 mg/mL), which is attributed to the stronger micellization tendency of star copolymer with a lower cac of about 0.006 mg/mL. Given that one Con A molecule binds with four glucose molecules [28,29], it can be concluded that about 7% of glucose units within star copolymer clustered with Con A, while 44% of glucose units within linear copolymer did [44]. This can be attributed to the fact that both the lower mobility and the higher spatial hindrance within star copolymers, to some extent, limited the clustering between sugar and Con A. This also suggests that the amount of lectin clustering might be controlled by adjusting the macromolecular architecture of copolymer.

3.4. *In vitro drug release from nimodipine-loaded nanoparticles*

Using the dialysis method, nimodipine was selected as a model hydrophobic drug to incorporate into the sugar-installed nanoparticles. Compared with linear $LPCL_{28}$-$PGAMA_{28}$ with a drug-loading efficiency of 42.4%, star PAMAM–PCL_{28}-$PGAMA_{28}$ showed a higher drug-loading efficiency (74.1%). This can be explained by the following two facts. One is that star copolymer had some hydrophobic cavities useful for the encapsulation of nimodipine drug via hydrophobic interactions [36–38]. The other is that the star copolymer with a lower cac had a relatively quicker micellization process compared with linear counterpart, which resulted in less drug unencapsulated in dialysis solution [2]. This result suggests that the star architecture of copolymer was beneficial for the encapsulation of hydrophobic drug within nanoparticles. The drug release behavior of the nimodipine-loaded nanoparticles at 37 °C is shown in Fig. 10. The star copolymers nanoparticles gave a less burst release (about 15% drug was released within 24 h), while about 45% drug was released from linear counterpart within 24 h. The large burst release of linear copolymer nanoparticles can be attributed to the following reasons. One is that a certain amount of nimodipine drug was not compactly encapsulated into the hydrophobic PCL core during the micellization process, and the other is that the drug-loaded nanoparticles have large surface areas because of their minimal diameter [45]. These two factors resulted in the fast release of about 45% nimodipine from the drug-loaded nanoparticles. However, for the star copolymer nanoparticles, hydrophobic nimodipine was probably encapsulated into the inner

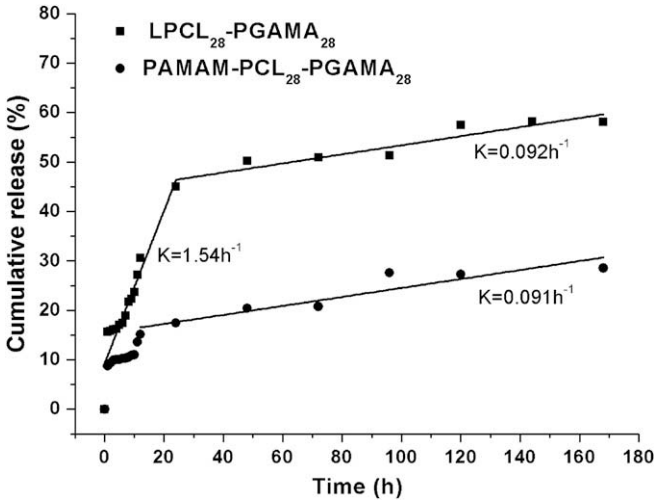

Fig. 10. *In vitro* drug-release profile of the nimodipine-loaded nanoparticles from both linear $LPCL_{28}$–$PGAMA_{28}$ and dendritic $PAMAM–PCL_{28}–PGAMA_{28}$ copolymers.

cavities of copolymer, inducing the less burst release. Then, these drug-loaded nanoparticles gave a slow drug-release rate (K) of about 0.09 h^{-1} from one day to seven days. This was mainly controlled by the drug diffusion from nanoparticles, which was associated with enhanced water uptake by hydrophilic glycopolymer shell at 37 °C. In conclusion, comparing with linear counterpart, the star PCL/glycopolymer biohybrid with a dendrimer core might provide a platform for the fabrication of sugar-installed nanoparticles with tunable clustering ability, good drug-loading efficiency, and controlled drug-release profile useful for targeted drug delivery system.

4. Conclusions

Star PAMAM–PCL–PGAMA biohybrids with a dendrimer core were successfully synthesized from the ROP of CL using a dendritic PAMAM–OH initiator followed by the direct ATRP of unprotected GAMA glycomonomer. The self-assembly and the biomolecular binding of PAMAM–PCL–PGAMA with Con A lectin were evidenced in detail by means of NMR, UV–vis, DLS, and TEM. Large compound aggregates and vesicles self-assembled from these biohybrids in aqueous solution, and they had a biodegradable PCL core surrounded by a multivalent glycopolymer shell. Moreover, these copolymers demonstrated specific biomolecular binding with Con A compared with BSA, and the amount of lectin clustering might be controlled by adjusting the macromolecular architecture. Furthermore, star copolymer nanoparticles showed a higher drug-loading efficiency and less burst release compared with linear counterpart. Consequently, these star PCL/glycopolymer biohybrids with a dendrimer core potentially provide a platform for the fabrication of sugar-installed nanoparticles with tunable clustering ability, good drug-loading efficiency, and controlled drug-release profile useful for targeted drug delivery system.

Acknowledgment

The authors are greatly grateful for the financial support of the National Natural Science Foundation of China (20674050 and 20874058) and Shanghai Leading Academic Discipline Project (B202), and many thanks for the assistance of Instrumental Analysis Center of SJTU.

Appendix. Supplementary data

Supplementary data associated with this article can be found in the online version, at doi:10.1016/j.polymer.2009.07.017.

References

[1] Batrakova EV, Kabanov AV. J Control Release 2008;130:98–106;
Ganta S, Devalapally H, Shahiwala A, Amiji M. J Control Release 2008;126:187–204.
[2] Discher DE, Ahmed F. Annu Rev Biomed Eng 2006;8:323–41.
[3] Osada K, Kataoka K. Adv Polym Sci 2006;202:113–53.
[4] Kita-Tokarczyk K, Grumelard J, Haefele T, Meier W. Polymer 2005;46:3540–63.
[5] Fujiwara T, Kimura Y. Macromol Biosci 2002;2:11–23.
[6] Bae YH. J Control Release 2008, doi:10.1016/j.jconrel.2008.09.074.
[7] Park JH, Lee S, Kim JH, Park K, Kim K, Kwon IC. Prog Polym Sci 2008;33:113–37.
[8] Peer D, Karp JM, Hong S, Farokhzad OC, Margalit R, Langer R. Nat Nanotechnol 2007;2:751–60.
[9] Noh T, Kook YH, Park C, Youn H, Kim H, Oh ET, et al. J Polym Sci Polym Chem 2008;46:7321–31.
[10] Chabre YM, Roy R. Curr Topics Med Chem 2008;8:1237–85.
[11] Kiessling LL, Gestwicki JE, Strong LE. Angew Chem Int Ed 2006;45:2348–68.
[12] Yasugi K, Nakamura T, Nagasaki Y, Kato M, Kataoka K. Macromolecules 1999;32:8024–32.
[13] Liang YZ, Li ZC, Li FM. New J Chem 2000;24:323–8;
Lu FZ, Meng JQ, Du FS, Li ZC, Zhang BY. Macromol Chem Phys 2005;206:513–20.
[14] Yamada K, Minoda M, Fukuda T, Miyamoto T. J Polym Sci Polym Chem 2001;39:459–67.
[15] Chen YM, Wulff G. Macromol Rapid Commun 2002;23:59–63.
[16] Bes L, Angot S, Limer A, Haddleton DM. Macromolecules 2003;36:2493–9.
[17] Narain R, Armes SP. Biomacromolecules 2003;4:1746–58.
[18] You LC, Schlaad H. J Am Chem Soc 2006;128:13336–7.
[19] Suriano F, Coulembier O, Degee P, Dubois P. J Polym Sci Polym Chem 2008;46:3662–72.
[20] Xiao NY, Li AL, Liang H, Lu J. Macromolecules 2008;41:2374–80.
[21] Dai XH, Dong CM, Yan D. J Phys Chem B 2008;112:3644–52;
Dai XH, Dong CM. J Polym Sci Polym Chem 2008;46:817–29;
Zhou W, Dai XH, Dong CM. Macromol Biosci 2008;8:268–78.
[22] Dong CM, Guo YZ, Qiu KY, Gu ZW, Feng XD. J Control Release 2005;107:53–64.
[23] McKee MG, Wilkes GL, Long TE. Prog Polym Sci 2005;30:507–39.
[24] Haag R. Angew Chem Int Ed 2004;43:278–82.
[25] Hua Y, Jiang XQ, Ding Y, Zhang LY, Yang CZ, Zhang JF, et al. Biomaterials 2003;24:2395–404.
[26] Newkome GR, Baker GR, Arai S, Saunders MJ, Russok PS, Theriot J, et al. J Am Chem Soc 1990;112:8458–65.
[27] Park SY, Han BR, Na KM, Han DK, Kim SC. Macromolecules 2003;36:4115–24.
[28] Khan MI, Mandal DK, Brewer CF. Carbohydr Res 1991;213:69–77.
[29] Wolfenden ML, Cloninger MJ. Bioconjugate Chem 2006;17:958–66.
[30] Narumi A, Kakuchi T. Polym J 2008;40:383–97.
[31] Miura Y. J Polym Sci Polym Chem 2007;45:5031–6.
[32] Spain SG, Gibson MI, Cameron NR. J Polym Sci Polym Chem 2007;45:2059–72.
[33] Nicolas J, Mantovani G, Haddleton DM. Macromol Rapid Commun 2007;28:1083–111.
[34] Cunliffe D, Pennadam S, Alexander C. Eur Polym J 2004;40:5–25.
[35] Okada M. Prog Polym Sci 2001;26:67–104.
[36] Yuan WZ, Yuan JY, Zheng SX, Hong XY. Polymer 2007;48:2585–94.
[37] Lowe AB, Wang R. Polymer 2007;48:2221–30.
[38] Sánchez-Chaves, Ruiz MC, Cerrada ML, Fernández-García M. Polymer 2008;49:2801–7.
[39] Miao ZM, Cheng SX, Zhang XZ, Wang QR, Zhuo RX. J Biomed Mater Res Part B Appl Biomater 2007;81B:40–9.
[40] Cai Q, Zhao Y, Bei J, Xi F, Wang S. Biomacromolecules 2003;4:828–34.
[41] Tomalia DA. Prog Polym Sci 2005;30:294–324.
[42] Zhang L, Eisenberg A. J Am Chem Soc 1996;118:3168–81.
[43] Yu Y, Eisenberg A. J Am Chem Soc 1997;119:8383–4.
[44] The highest value of ConA clustering was equivalent to that of PAMAM–PCL–PGAMA, and the binding glucose unit percent within copolymer (G) can be calculated by equation: $G = [(W_{ConA}/M_{n,\ ConA}) \times 4]/[(W_{copolymer}/M_{n,\ copolymer}) \times DP_{PGAMA}] \times 100\%$, where $M_{n,\ ConA} = 102\,000$.
[45] Dong Y, Feng SS. J Biomed Mater Res 2006;78A:12–9.